Watching Vibrational Energy Transfer in Liquids with Atomic Spatial Resolution

Zhaohui Wang, Andrei Pakoulev, Dana D. Dlott*

Ultrafast spectroscopy was used to study vibrational energy transfer between vibrational reporter groups on different parts of a molecule in a liquid. When OH stretching vibrations of different alcohols were excited by mid-infrared laser pulses, vibrational energy was observed to move through intervening CH_2 or CH groups, taking steps up and down in energy, ending up at terminal CH_3 groups. For each additional CH_2 group in the path between OH and CH_3, the time for vibrational energy transfer increased by about 0.4 picosecond.

The movement of vibrational energy within and between molecules plays an important role in virtually all condensed-phase chemical processes (*1*). Here we report real-time observations of vibrational energy flow across molecules of different lengths. Vibrational energy transfer (VET) was observed between vibrational reporter groups (atomic groups with nearly local-mode vibrational excitations) on different parts of a molecule in a liquid. The distances between vibrational donors and acceptors were varied in units of one carbon-carbon bond length (~1.5 Å), so that the distance dependence of VET could be investigated.

A mid-infrared (mid-IR) pulse 0.6 ps in duration was used to excite the OH stretching transition of a series of different liquid alcohols at ambient temperature in a flowing jet. The alcohols have the general structure CH_3-R-OH, where R is a hydrocarbon moiety. A 0.7-ps visible probe pulse (25 cm^{-1} spectral bandwidth) generated spontaneous anti-Stokes Raman scattering that was detected with a multichannel spectrograph (*2*, *3*). Time-dependent pump-induced changes in anti-Stokes intensities were used to monitor the loss of vibrational excitation from OH and the arrival of vibrational excitation at a terminal CH_3 group. This IR-Raman technique and related IR-IR techniques (*4–8*) have been used to study ethanol and other alcohols in the past, but prior studies have not had the time resolution and sensitivity needed to observe the distance dependence of VET across molecular dimensions.

Although VET from a donor to an acceptor on another part of a molecule is reminiscent of electronic energy transfer between dye molecules anchored to different parts of a molecule, it is fundamentally quite different. Electronic energy transfer typically involves through-space interactions, such as a dipole-dipole interaction in the case of Förster transfer (*9*), between electronic states of molecules with overlapping emission and absorption spectra. Through-space VET is not expected to be significant between OH and CH stretching transitions located a few angstroms apart, because typical dipole moments and spectral overlap factors do not yield energy transfer rates remotely competitive with the <10-ps nonradiative lifetimes. As shown here, VET is fundamentally mechanical and occurs via a through-bond interaction involving solvent-assisted anharmonic coupling (*10*).

A diagram of the relevant levels (*11*, *12*) for the examples of ethanol CH_3CH_2OH and 1-propanol $CH_3(CH_2)_2OH$ is shown in Fig. 1. These levels are as follows: OH stretching ν_{OH}; two CH stretches of each intervening CH_2 group, the symmetric $\nu_s(CH_2)$ and asymmetric $\nu_a(CH_2)$; and three CH stretches of terminal CH_3 groups, the symmetric $\nu_s(CH_3)$ and the (doubly degenerate) asymmetric $\nu_a(CH_3)$. Stretching excitations of hydrogen-bonded moieties such as OH in methanol (*13*, *14*) or water (*15*) may hop among nearby molecules during the OH stretching lifetime, but that should not have much effect on the intramolecular transfer to CH_2 and CH_3 stretching vibrations. Also, there is often considerable mixing between CH stretching and the first overtones of CH bending vibrations $2\delta(CH_2)$ and $2\delta(CH_3)$. Because interactions between CH bending excitations on adjacent carbon atoms are generally larger than between CH stretching excitations, the extent of this mixing plays an important role in determining the rate of stretch excitation transport between neighboring atomic groups.

Because of the considerable energy mismatch for energy transfer from ν_{OH} to ν_{CH}, about 300 cm^{-1} in the present work, the $\nu_{OH} \rightarrow \nu_{CH}$ process requires a solvent bath (*1*, *10*). In a liquid at ambient temperature, steps up or down in energy of a few hundred cm^{-1} are possible (*10*), because the average thermal energy of the bath is ~200 cm^{-1}. Energy flow of ν_{CH} excitations down hydrocarbon chains isolated from a thermal bath is possible, but only if ν_{CH} is excited in a higher overtone region where the density of states (*16*) is much higher than in the fundamental region (*17*).

Broadly speaking, there are two ways for excitation energy to be transferred from ν_{OH} to a terminal CH_3 group. In a vibrational cascade (*16*), vibrational excitation percolates down the energy levels. If the vibrational cascade were dominant, Fig. 1 shows that ν_{OH} decay would first excite the higher energy "a" states $\nu_a(CH_3)$ and $\nu_a(CH_2)$ and then the lower energy "s" states $\nu_s(CH_2)$ and $\nu_s(CH_3)$. [$\nu_a(CH_2)$ is not shown explicitly in Fig. 1 because this transition is not seen in the Raman or IR spectra of these alcohols.] In through-bond transfer, vibrational excitation would run from OH across the intervening atomic groups, first to CH_2 and then to CH_3. Figure 1 shows that energetically, the through-bond process involves a first step down in energy from ν_{OH} to $\nu_s(CH_2)$, followed by steps up in energy to $\nu_s(CH_3)$ and $\nu_a(CH_3)$.

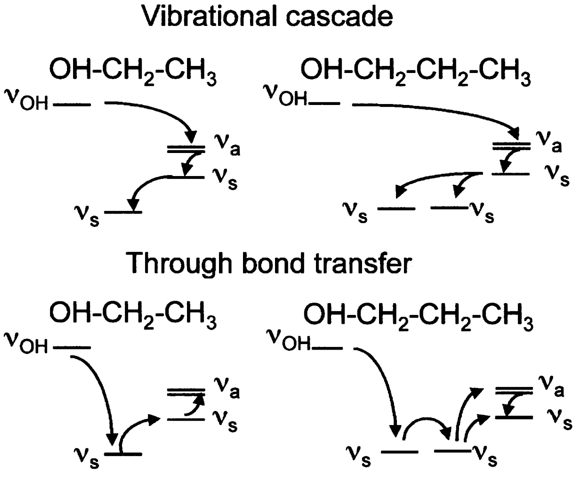

Fig. 1. Energy-level diagrams for VET from OH to CH stretching vibrations of ethanol (left) and 1-propanol (right). Not shown are the lower energy bend and stretch vibrations that are the dominant energy relaxation pathways for excited OH and CH stretching excitations. **(Top)** If vibrational energy moved downward through the energy levels (vibrational cascade), methyl CH_3 stretching vibrations would be populated before methylene CH_2 vibrations. **(Bottom)** If through-bond VET were dominant, vibrational energy would move through the intervening methylene vibrations before reaching the methyl group.

School of Chemical Sciences, University of Illinois at Urbana-Champaign, Box 01–6 CLSL, 600 South Mathews Avenue, Urbana, IL 61801, USA.

*To whom correspondence should be addressed. E-mail: Dlott@scs.uiuc.edu

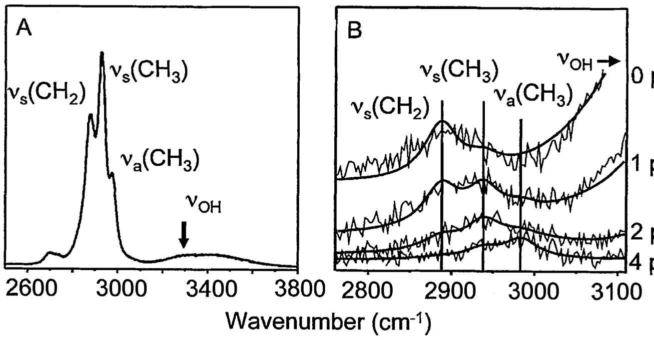

Fig. 2. (**A**) Spontaneous Stokes Raman spectrum of ethanol (liquid, 295 K) showing the OH stretch and CH_3 and CH_2 stretching vibrations. The arrow indicates the wave number of the mid-IR pump pulses used here. (**B**) Anti-Stokes transient spectra. The computer-generated smooth curves use parameters taken from the Stokes Raman spectrum with variable amplitude factors. The anti-Stokes intensities are proportional to the instantaneous vibrational populations. The OH excitations pumped by the laser are to the right of the displayed spectra. No more than 1 to 2% of the OH stretch excitations are transferred to CH stretch excitations. Vibrational excitation is observed to flow from OH, first to CH_2 and subsequently uphill in energy to CH_3, as indicated in the through-bond transfer scheme in Fig. 1.

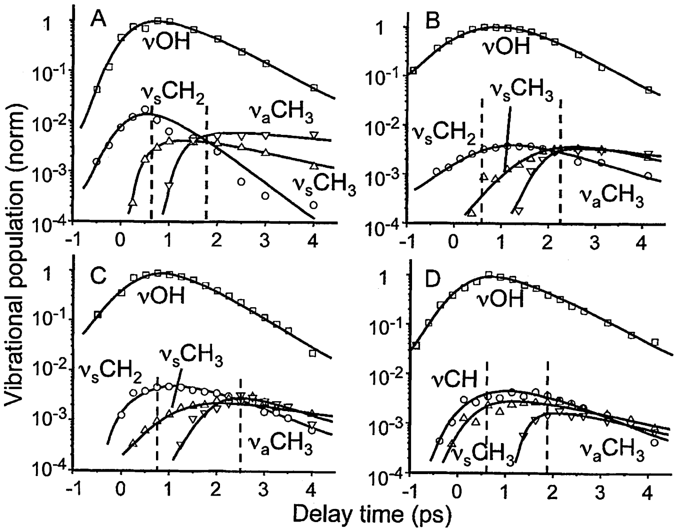

Fig. 3. Time-dependent populations after OH stretching excitation of OH and CH stretching vibrations of ethanol (**A**), 1-propanol (**B**), 1-butanol (**C**), and 2-propanol (**D**). In (A) to (C), energy was observed to flow from OH to CH_2 to CH_3. The vertical line pair in each panel marks the peak of the OH and CH_3 (a-state) populations. The time constant for OH → CH_3 (a-state) transfer increases by about 0.4 ps for each additional intervening CH_2 group. In (D), energy was observed to flow from OH to CH and then to CH_3. This three-atom-group path is almost the same length as in ethanol and is shorter than in 1-propanol and 1-butanol.

The Stokes Raman spectrum of ethanol in Fig. 2, obtained with our 0.7-ps visible laser pulses, shows that we can clearly resolve the OH, CH_2, and CH_3 stretching transitions (*12*). The anti-Stokes transient spectra in Fig. 2 are obtained at the indicated times after excitation of ν_{OH} at 3300 cm^{-1}, near the center of the broad mid-IR absorption. In transient anti-Stokes spectroscopy, the instantaneous intensity of each transition is proportional to the product of the occupation number (that is, the excited state population) and the Raman cross-section (*18*). The Raman cross-section for ν_{OH} is about 10 times smaller than for ν_{CH}. Initially (near time = 0), there appeared a large excitation of ν_{OH}. The maximum signal from OH stretching excitations (off the right edge of Fig. 2) is more than five times greater than the signal from CH stretching. Thus, just a few percent of the ν_{OH} excitations pumped by the laser were transferred to CH stretching. In the first picosecond, the predominant product of ν_{OH} decay in the ν_{CH} region is the CH_2 stretch $\nu_s(CH_2)$. Subsequently, the energy in the CH_2 group moves uphill in energy from $\nu(CH_2)$ to $\nu(CH_3)$. The data in Fig. 2 clearly distinguish between the two possibilities illustrated in Fig. 1. Energy transfer from ν_{OH} to $\nu(CH_3)$ in ethanol moves from OH, first to CH_2 and then to CH_3. Thus, this energy transfer occurs via the through-bond mechanism as opposed to a vibrational cascade down the energy levels from OH to CH_3 to CH_2.

Transient spectra such as those in Fig. 2 were fitted by a computer program that determined the relative intensities of the OH and CH stretching transitions (*19*, *20*). Combined with Raman cross-sections from Stokes spectra, these intensities gave the time-dependent vibrational populations (normalized to the peak ν_{OH} population) shown in Fig. 3. The ethanol data in Fig. 3A show that ν_{OH} decay first populated $\nu_s(CH_2)$, then $\nu_s(CH_3)$, and finally $\nu_a(CH_3)$. In order to determine a rough time constant for energy transfer from ν_{OH} to $\nu_s(CH_3)$ without resorting to a substantial amount of modeling, we drew two markers in each panel of Fig. 3 to indicate the time of the peak ν_{OH} population and the peak $\nu_a(CH_3)$ population. The time interval between the markers for ethanol is 1.0 ps.

Vibrational energy flow in 1-propanol $CH_3(CH_2)_2OH$ (Fig. 3B), 1-butanol $CH_3(CH_2)_3OH$ (Fig. 3C), and 2-propanol $(CH_3)_2CHOH$ (Fig. 3D) was also studied. In 1-propanol and 1-butanol, we could not resolve multiple CH_2 transitions, so we could not monitor energy flow between adjacent CH_2 groups. In 1-propanol, as in ethanol, ν_{OH} decay first populates the CH_2 stretching excitations, followed by stretching excitations of the terminal CH_3 group. However, as indicated by the markers in Fig. 3B, VET across the molecule took longer in 1-propanol (1.4 ps) than in ethanol. In 1-butanol, energy flow from OH to a terminal CH_3 group must pass through three intervening CH_2 groups. Figure 3C shows that energy flow from OH to the terminal CH_3 group took the longest time of all, 1.7 ps. Thus, to a rough approximation, adding an additional CH_2 group increased the time for vibrational flow from one end of an alcohol molecule to the other by about 0.4 ps. In 2-propanol, energy flowing from OH to a terminal CH_3 passes through only a single intervening CH atomic group. The markers in Fig. 3D show that the time for energy flow from OH to CH_3 in 2-propanol was almost exactly the same as in ethanol: 1.0 ps. The efficiency of energy transfer through CH in 2-propanol, where the intervening group has only one CH stretch excitation, was about one-third the efficiency of energy transfer through CH_2 in ethanol, where the intervening group has two CH stretch excitations.

Figure 4 shows a comparison between 1-butanol CH_3-$(CH_2)_3$-OH and *tert*-butanol $(CH_3)_3COH$. In the 1-butanol data in Fig. 4A, some CH stretch excitations were observed. These were produced by VET from the OH stretch pumped by a mid-IR laser pulse. In the *tert*-butanol data (Fig. 4B), essentially no CH stretch excitations were produced by OH stretch pumping. In *tert*-butanol, there are no CH stretching states on the carbon atom between OH and CH_3. Thus, Fig. 4 strongly indicates the dominance of through-bond VET. The lack of a CH stretching transition on the central carbon atom chokes off energy transfer from OH to the terminal CH_3 groups.

Carbon-carbon bond lengths in unsaturated molecules are typically ~1.5 Å, so a 0.4-ps time constant for VET across a CH_2 group roughly corresponds to a velocity of 375 m/s. That velocity is relatively high, about 10% greater than Mach 1, but it is

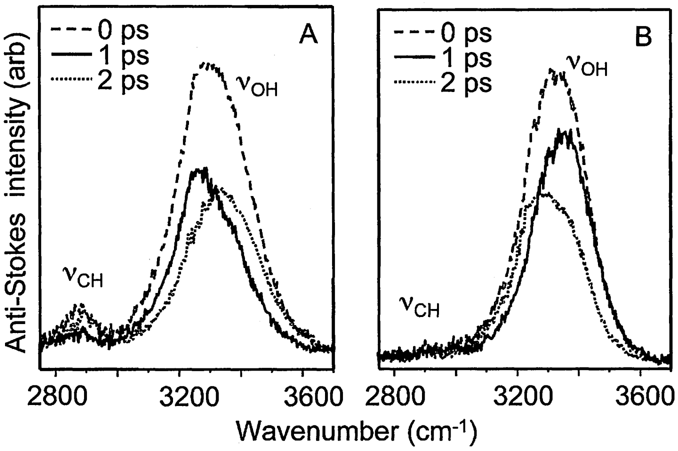

Fig. 4. Transient anti-Stokes spectra after OH stretch pumping, for 1-butanol and *tert*-butanol. (**A**) In 1-butanol, less than 1% of OH stretching excitations are transferred to CH_2 and CH_3 stretching excitations (the Raman cross-section for OH stretching is about 10 times smaller than for CH stretching). (**B**) In *tert*-butanol, no energy transfer is observed from OH to CH stretching. The central carbon atom, which has no CH stretching excitations, chokes off through-bond energy transfer from OH to CH_3.

only about one-third the speed of sound in ethanol (*21*). The overall efficiency for VET from OH to $\nu_a(CH_3)$ states is poor. In ethanol, the instantaneous population of stretching excitations on the terminal CH_3 was never more than about 0.7% of the OH stretch (Fig. 3A), and this efficiency dropped off by about a factor of 2 for each CH_2 added to the chain. That is because at the same time as vibrational energy is moving from OH to CH_3, it is also disappearing into lower energy OH and CH bending and CO stretching vibrations in the 1000 to 1500 cm^{-1} range (*20*), which is not discussed here. Differences in stretching-to-bending transition rates for the different OH, CH, CH_2, and CH_3 groups studied here and the competition between these rates and the rates of intermolecular transfer down the chain account in part for the different absolute vibrational populations of these groups seen in Fig. 3. It would be interesting if we could find other useful vibrational reporter groups with longer lifetimes, such as $C\equiv N$ (*22*) or aromatic ring-stretching vibrations (*23*), and intervening groups that are better conductors of vibrational energy, so that these studies could be extended to larger molecules and longer distances.

References and Notes

1. G. A. Voth, R. M. Hochstrasser, *J. Phys. Chem.* **100**, 13034 (1996).
2. L. K. Iwaki, J. C. Deàk, S. T. Rhea, D. D. Dlott, in *Ultrafast Infrared and Raman Spectroscopy*, M. D. Fayer, Ed. (Marcel Dekker, New York, 2000).
3. J. C. Deàk, L. K. Iwaki, D. D. Dlott, *Opt. Lett.* **22**, 1796 (1997).
4. E. J. Heilweil, M. P. Casassa, R. R. Cavanagh, J. C. Stephenson, *J. Chem. Phys.* **85**, 5004 (1986).
5. R. Laenen, C. Rauscher, *Chem. Phys. Lett.* **274**, 63 (1997).
6. S. Woutersen, U. Emmerichs, H. J. Bakker, *J. Chem. Phys.* **107**, 1483 (1997).
7. R. Laenen, K. Simeonidis, *Chem. Phys. Lett.* **299**, 589 (1999).
8. R. Laenen, C. Rauscher, A. Laubereau, *J. Phys. Chem. A* **101**, 3201 (1997).
9. T. Förster, *Ann. Phys.* **6**, 55 (1948).
10. V. M. Kenkre, A. Tokmakoff, M. D. Fayer, *J. Chem. Phys.* **101**, 10618 (1994).
11. B. Schrader, *Raman/Infrared Atlas of Organic Compounds* (VCH, Weinheim, Germany, ed. 2, 1989).
12. J.-P. Perchard, M.-L. Josien, *J. Chim. Phys.* (*Paris*) **65**, 1834 (1968).
13. J. C. Deàk, L. K. Iwaki, S. T. Rhea, D. D. Dlott, *J. Raman Spectrosc.* **31**, 263 (2000).
14. X. Hong, S. Chen, D. D. Dlott, *J. Phys. Chem.* **99**, 9102 (1995).
15. S. Woutersen, H. J. Bakker, *Nature* **402**, 507 (1999).
16. A. Nitzan, S. Mukamel, J. Jortner, *J. Chem. Phys.* **63**, 200 (1975).
17. J. S. Hutchinson, W. P. Reinhardt, J. T. Hynes, *J. Chem. Phys.* **79**, 4247 (1983).
18. A. Laubereau, W. Kaiser, *Rev. Mod. Phys.* **50**, 607 (1978).
19. L. K. Iwaki, D. D. Dlott, *Chem. Phys. Lett.* **321**, 419 (2000).
20. ———, *J. Phys. Chem. A* **104**, 9101 (2000).
21. D. R. Lide, Ed., *Handbook of Chemistry and Physics 81st Edition* (CRC, Cleveland, OH, 1996).
22. J. C. Deàk, L. K. Iwaki, D. D. Dlott, *J. Phys. Chem.* **102**, 8193 (1998).
23. L. K. Iwaki, J. C. Deàk, S. T. Rhea, D. D. Dlott, *Chem. Phys. Lett.* **303**, 176 (1999).
24. This material is based on work supported by NSF under award number DMR-0096466, by the Air Force Office of Scientific Research under contract F49620-00-1-0049, and by the Army Research Office contract DAAD19-00-1-0036.

26 February 2002; accepted 24 April 2002

Structure of the 8200-Year Cold Event Revealed by a Speleothem Trace Element Record

James U. L. Baldini,[1]* Frank McDermott,[1] Ian J. Fairchild[2]

Abrupt first-order shifts in strontium and phosphorus concentrations in stalagmite calcite deposited in western Ireland during the 8200-year event (the major cooling episode 8200 years before the present) are interpreted as responses to a drier climate lasting about 37 years. Both shifts are centered on 8330 ± 80 years before the present, coinciding with a large oxygen isotope anomaly and a change in the calcite petrography. In this very high resolution (monthly) record, antipathetic second-order oscillations in phosphorus and strontium reveal decreased growth rates and increased rainfall seasonality. Growth rate variations within the event reveal a two-pronged structure consistent with recent model simulations.

The 8200-year event is widely regarded as the strongest Holocene cooling episode, with clear expressions in Greenland (*1, 2*), the North Atlantic (*3*), Europe (*4–11*), North America (*12–14*), North Africa (*15*), and the Venezuelan Cariaco Basin (*16*). Decreased snow accumulation rates, lower levels of atmospheric methane, and increased atmospheric dust and sea-salt loadings indicate widespread dry conditions (*17, 18*). Explanations usually involve a perturbation of the North Atlantic thermohaline circulation (THC) by increased freshwater inputs associated with the decay of the Laurentide ice sheet (*6, 19*). A high-resolution global circulation model (GCM) indicates that a freshwater pulse of a magnitude similar to that associated with the catastrophic drainage of the large proglacial lakes Agassiz and Ojibway could have produced the 8200-year event, including a very brief warming episode within the event (*20*).

Crucial unresolved questions are whether the cooling occurred as a single event or as a more complex multipulse episode involving partial recovery, and whether the cooling resulted in enhanced seasonality in mid-latitude temperate regions. The latter is important because it may affect the detection of the event by some proxies such as tree rings. The coarse resolution of the available climate records has hampered investigation of these issues. Here, we present a very high resolution trace element record for

---

[1] Department of Geology, University College Dublin, Belfield, Dublin 4, Ireland. [2] School of Earth Sciences and Geography, Keele University, Staffordshire ST5 5BG, UK.

*To whom correspondence should be addressed. E-mail: james.baldini@ucd.ie